

ARTICLE



Genetic alterations in gastric amphicrine carcinomas and comparison with gastric mixed neuroendocrine-non-neuroendocrine neoplasms

Lin Sun^{1,3}, Chao Wang^{1,3}, Jingyi Zhang¹, Bing Shao¹, Shuai Zhao¹, Yuhong Guo¹, XiangChun Li²  and Yan Sun¹ 

© The Author(s), under exclusive licence to United States & Canadian Academy of Pathology 2021

Gastric amphicrine carcinoma, in which endocrine and epithelial cell features are present within the same cells, is often confused with gastric mixed neuroendocrine-non-neuroendocrine neoplasm (MiNEN). In this study, we performed high-resolution copy number (CN) profiling and whole exome sequencing (WES) of formalin-fixed and paraffin-embedded (FFPE) tissues from eight gastric amphicrine carcinomas and compared the molecular features with those of the adenocarcinoma and neuroendocrine carcinoma (NEC) components of eight gastric MiNENs. The most frequent high-level CN variant was a gain of 20q13.12–20q13.2, which was found in five gastric amphicrine carcinomas. Amplifications of *MYT1*, *NTSR1*, and *ZBTB46* located in this region were demonstrated by qPCR and immunohistochemistry. The CN characteristics of gastric amphicrine carcinomas were different from those of MiNENs in hierarchical clustering analysis, suggesting that amphicrine carcinoma is a separate entity from MiNEN. Moreover, the CN level of C5 (complement C5) was higher in amphicrine carcinoma than in both the adenocarcinoma and the NEC component of MiNENs, suggesting that amphicrine carcinomas might benefit more from C5 inhibitors than MiNENs. WES showed frequent somatic mutations of *TP53* (37.5%, 3/8) and *APC* (25.0%, 2/8) in amphicrine carcinoma. There were no specific mutation characteristics to distinguish amphicrine carcinoma from MiNEN. An integrated KEGG pathway analysis showed that the estrogen signaling pathway was enriched in amphicrine carcinomas, which might be associated with the high morbidity of male patients. In summary, our study revealed the unique CN and mutation characteristics of gastric amphicrine carcinoma and differentiated these characteristics from those of MiNENs. These data provide a foundation for further studies on the development and progression of amphicrine carcinoma.

Modern Pathology (2022) 35:808–815; <https://doi.org/10.1038/s41379-021-00978-5>

INTRODUCTION

The term “amphicrine” was introduced to describe a cell displaying exocrine and endocrine differentiation simultaneously¹. Almost more than 30 years ago, Lewin² proposed a simple nomenclature for dividing mixed exocrine-neuroendocrine tumors into three groups: mixed or composite tumors, collision tumors, and amphicrine tumors. Although the three types of tumors possess both exocrine and endocrine features, composite or collision tumors show exocrine and endocrine features in separate tumor cells, while amphicrine tumors display exocrine and neuroendocrine differentiation in the same cells. For a long time, amphicrine carcinoma has been regarded as a subtype of mixed exocrine-neuroendocrine tumors^{3, 4}. According to its grade of malignancy, amphicrine carcinoma is classified as an intermediate-grade mixed neuroendocrine-non-neuroendocrine neoplasm (MiNEN) or a mixed adenocarcinoma-well differentiated neuroendocrine tumor (NET)^{3, 4}. However, in 2019, the 5th edition of the WHO classification of digestive system tumors removed reference to amphicrine carcinoma among MiNENs without any comments⁵. Uccella and La

Rosa even considered discouraging the inclusion of amphicrine neoplasms in the concept of MiNEN for both biological and clinical reasons⁵. Due to its rare incidence, there have been few studies on the clinicopathology and molecular characteristics of amphicrine carcinoma, which hampers the understanding, diagnosis, and treatment of this tumor.

To gain a better understanding of the biological properties of this tumor, we histologically verified gastric amphicrine carcinoma in our center and analyzed its clinicopathological features. Then, we performed genome-wide copy number variation (CNV) and whole exome sequencing (WES) analyses on gastric amphicrine carcinoma and compared it with the adenocarcinoma and neuroendocrine carcinoma (NEC) components of gastric MiNENs. Based on the CNV, mutation characteristics, and protein expression, we identified novel chromosome regions and genes unique to amphicrine carcinoma, which highlights the molecular characteristics of gastric amphicrine carcinomas and the genetic commonalities and differences between this tumor and the two components of MiNENs. Our study outlines the molecular

¹Department of Pathology, Tianjin Medical University Cancer Institute and Hospital, National Clinical Research Center for Cancer, Key Laboratory of Cancer Prevention and Therapy, Tianjin, Tianjin's Clinical Research Center for Cancer, Tianjin, China. ²Department of Epidemiology and Biostatistics, Tianjin Medical University Cancer Institute and Hospital, National Clinical Research Center for Cancer, Tianjin's Clinical Research Center for Cancer, Key Laboratory of Cancer Prevention and Therapy, Tianjin, China. ³These authors contributed equally: Lin Sun, Chao Wang. email: sunyan@tjmuch.com

Received: 31 July 2021 Revised: 30 October 2021 Accepted: 12 November 2021

Published online: 27 November 2021

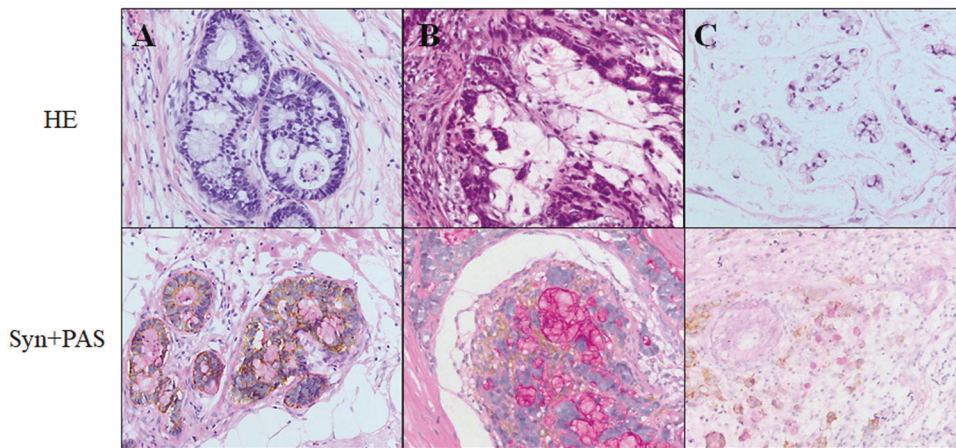


Fig. 1 Representative histological images and Syn/Periodic Acid-Schiff (PAS) double staining images of gastric amphicrine carcinoma. **a** Moderately differentiated amphicrine carcinoma presented as a glandular duct-like structure (HE, 400×) with both PAS-positive mucus and Syn-positive neuroendocrine granules in the cytoplasm (double staining, 400×). **b** Poorly differentiated amphicrine carcinoma presented as a solid nest-like structure or scattered tumor cells with mucus lake formation (HE, 400×). Mucus was visible in the intercellular space, and Syn-positive neuroendocrine granules were observed in the cytoplasm of tumor cells (double staining, 400×). **c** Poorly differentiated signet-like amphicrine carcinoma presented as clustered or scattered signet-like cells (HE, 400×) with intracellular mucus and Syn-positive neuroendocrine granules (double staining, 400×).

characteristics of gastric amphicrine carcinoma, provides clues to define this rare tumor, and reveals that gastric amphicrine carcinoma is more dissimilar in CN gain to the NEC component of MiNENs and less dissimilar to the adenocarcinoma component of MiNENs.

MATERIALS AND METHODS

Patients and samples

We collected samples from 8 patients with gastric amphicrine carcinoma who underwent surgery at Tianjin Medical University Cancer Institute and Hospital from March 2011 to June 2020. The diagnosis of gastric amphicrine carcinoma was agreed upon by two pathologists after they reviewed all the hematoxylin and eosin, immunohistochemistry, and periodic acid Schiff (PAS)-stained sections. Details of the antibodies used are listed in Supplementary Table S1. The clinicopathological data and survival information were collected for all cases. This study was approved by the Institutional Review Board of Tianjin Medical University Cancer Institute and Hospital and is in compliance with the Helsinki Declaration.

Copy number variation analysis

Tumor samples and tumor-adjacent normal tissues were obtained from each case at the same time. DNA was extracted with a QIAamp DNA FFPE Tissue Kit according to the manufacturer's instructions (Qiagen, CA, USA) and quantified using agarose gel electrophoresis, a NanoDrop2000 spectrophotometer (Thermo Scientific, MA, USA), and a Qubit 2.0 fluorometer (Thermo Scientific, MA, USA).

CNV analysis was performed in eight gastric amphicrine carcinomas. The experimental procedures and cutoff values have been described in detail previously⁷. To compare the commonalities and differences between gastric amphicrine carcinoma and MiNEN, we collected all the genes and the median log₂ ratios from gastric amphicrine carcinoma and the adenocarcinoma and NEC components of MiNENs that we had obtained previously⁷. Hierarchical clustering was performed, and JAVA TreeView was used to draw heatmaps to visualize the clustering results.

Whole exome sequencing analysis

Whole exome sequencing (WES) was performed in 8 gastric amphicrine carcinomas, two components of 7 gastric MiNENs, and their tumor-adjacent normal tissues. A library was prepared with an Agilent SureSelect Human All Exon Kit, and sequencing was performed on an Illumina HiSeq according to the manufacturer's protocol. Details of the analysis software and database are listed in Supplementary Table S2.

Integrated analysis of genetic characteristics

Kyoto Encyclopedia of Genes and Genomes (KEGG) was used for pathway enrichment analysis of genes with somatic mutations and high-frequency CN variant genes of gastric amphicrine carcinomas and the two components of MiNENs. The results were visualized with the ClueGo plug-in of Cytoscape software (version 3.6.0). A *P* value < 0.05 was set as the cutoff criterion.

Quantitative real-time PCR, Sanger sequencing, and immunohistochemical staining

Quantitative real-time PCR (qPCR) for *MYT1*, *NTSR1*, and *ZBTB46* was performed using a StepOnePlus Real-Time PCR System (Applied Biosystems, CA, USA). The primer information is listed in Supplementary Table S3. Details of the reaction mixture and analysis method have been described previously⁷.

DNA samples from amphicrine carcinomas were amplified to validate the somatic mutation of *TP53* (NM_000546) detected by whole exome sequencing using Sanger sequencing with a 3500 Genetic Analyzer (Thermo Scientific, MA, USA). The primers used for PCR are listed in Supplementary Table S3.

Immunohistochemical (IHC) staining was performed on 4- μ m sections from formalin-fixed and paraffin-embedded (FFPE) tumor tissues and normal control tissues to detect *MYT1*, *NTSR1*, and *ZBTB46* according to the established protocol. Details of the antibodies are listed in Supplementary Table S1.

Statistical analyses

Statistical analysis was performed with SPSS 22.0. Independent sample *t* tests of the median log₂ ratio of all genes from each sample were used to assess differences in CN characteristics between gastric amphicrine carcinoma and the two components of MiNENs. CN levels in each tumor sample and normal tissue were compared with paired *t* tests. A significant difference was considered when the *P* value < 0.05.

RESULTS

Clinicopathological characteristics and survival analysis of gastric amphicrine carcinomas

Eight gastric amphicrine carcinomas were identified based on typical morphology, IHC phenotype, PAS staining, and Syn/PAS double staining. Microscopically, 3 patients presented with moderately differentiated adenocarcinoma composed of glandular duct-like structures with mucus in the gland lumen and were simultaneously positive for the neuroendocrine marker Syn (Fig. 1A). Seven cases with poorly differentiated adenocarcinoma

Table 1. The clinicopathologic characteristics of eight gastric amphicrine carcinomas and eight gastric MiNENs.

No.	Sex/ Age	Site	Diagnosis	Differentiation	TNM stage	Adjuvant therapy	Status	Follow-up (Months)
1	M/60	Fundus	Amphicrine	Poor	T2N0M0	+	Alive, NED	45
2	M/58	Gastric body	Amphicrine	Moderate	T4aN1M0	+	Death, DOD	18
3	M/59	Cardia	Amphicrine	Poor	T3N1M0	+	Alive, NED	25
4	M/67	Cardia	Amphicrine	Poor (60%) and Moderate (40%)	T4aN1M0	+	Alive, NED	39
5	M/54	Gastric body	Amphicrine	Poor	T4aN2M0	+	Alive, AWD ^a	49
6	M/68	Angle	Amphicrine	Poor	T2N0M0	+	Alive, NED	56
7	M/30	Angle	Amphicrine	Poor	T3N0M0	–	Alive, NED	40
8	M/60	Antrum	Amphicrine	Poor (30%) and Moderate (70%)	T4aN3M0	–	Alive, NED	6
9	M/73	Cardia	MiNEN	ADC: Moderate; NEC: large cell	T4aN3aM0	+	Death, DOD	21
10	F/59	Antrum	MiNEN	ADC: Poor; NEC: large cell	T4bN3aM0	+	Death, DOD	23
11	F/52	Antrum	MiNEN	ADC: Moderate; NEC: large cell	T1N0M0	-	Alive, NED	46
12	M/60	Cardia	MiNEN	ADC: Moderate; NEC: large cell	T4aN2M0	+	Death, DOD	12
13	M/64	Gastric body	MiNEN	ADC: Moderate; NEC: large cell	T4aN3aM0	+	Death, DOD	5
14	M/52	Angle	MiNEN	ADC: Moderate; NEC: large cell	T1N1M0	+	Death, DOD	22
15	M/74	Antrum	MiNEN	ADC: Moderate; NEC: large cell	T4bN1M0	+	Death, DOD	30
16	M/50	Cardia	MiNEN	ADC: Moderate; NEC: large and small cell	T2N1M0	+	Alive, NED	33

Abbreviations: M, male; F, female; MiNEN, mixed neuroendocrine-non-neuroendocrine neoplasm; ADC, adenocarcinoma; NEC, neuroendocrine carcinoma; NED, no evidence of disease; DOD, death of disease; AWD, alive with disease.

^aliver metastasis was detected ten months after surgery.

presented as solid nest-like or scattered tumor cells with mucus in the intercellular space or inside the cell and were concurrently positive for Syn (Fig. 1B). In addition, signet-like cells were observed in 6 cases (Fig. 1C), and mucus lakes were formed in 3 cases (Fig. 1B, C).

All 8 patients were male, and the median age was 59.5 years (ranging from 30 to 68). The clinical presentation was unspecific, with symptoms ranging from abdominal discomfort or pain to sour regurgitation or emesis. The tumors were located throughout the stomach, and the gastric antrum/angle, found in three cases, was the most commonly involved region. All tumors presented an ulcerative nature with a median longest diameter of 4.25 cm (2.0–6.0 cm). Lymphatic metastasis was found in 5 patients at diagnosis. None of the patients presented with distant metastasis at diagnosis. According to the American Joint Committee on Cancer pathologic TNM staging system (eighth edition), 4 cases were classified as early stage (I or II) and 4 cases as late stage (III). Six patients received adjuvant therapy after surgery. Due to its rarity, there is no standard treatment protocol, and raltitrexed, platinum, fluorouracil, etoposide, irinotecan, temozolomide, and docetaxel have been used for different patients or in different treatment cycles. During the follow-up period, 2 patients presented recurrence or metastasis to the liver. At the end of follow-up, one patient died. The clinicopathologic features of these eight amphicrine carcinoma cases and the eight MiNENs for comparing genetic alterations are summarized in Table 1.

The landscape of copy number variations in gastric amphicrine carcinomas

CNV analysis was performed in 8 gastric amphicrine carcinomas using an OncoScan CNV Assay. Affected chromosome segments are shown in Fig. 2A. Gains of chromosome regions were detected at 1q21.1-q25.3, 2q31.1, 3p26.3-p12.2, 3q11.1-q29, 5p15.33-q11.1, 7p21.3-p11.1, 8p23.3-q24.3, 9q21.11-q34.3, 10p15.3-p15.1, 10q21.2, 12q13.3-q24.33, 13q12.2-q34, 14q13.3, 17q11.2-q25.3, 19p13.3-p12, 19q12-q13.43, 20p13-p11.21, and 20q11.22-q13.33; losses of

chromosome regions were detected at 2p16.1-p13.3, 9p24.1, 15q14–25.2, 16p13.3-p13.11, 16q11.2-q21, 17p13.1-p11.2, 17q12, and 22q11.23-q13.33; and these changes were identified in at least four cases.

We selected genes located in the above CNV regions to perform further analysis. The number of genes in the chromosome regions with gains was much greater than that in regions with losses (1720 vs. 439, $P = 0.003$). Taking a median \log_2 ratio ≥ 0.25 and CN status ≥ 2.5 as high-level copy number gains and a median \log_2 ratio ≤ -0.25 and CN status ≤ 1.5 as high-level copy number losses, 20q13.12-q13.2 (detected in five cases) was the most frequent high-level copy number gain region, followed by 5p15.3-q11.1 (detected in four cases). Further analysis of the genes at 20q13.12-q13.2 showed that the mRNA expression levels of many genes in this region, such as *MYT1*, *NTSR1*, and *ZBTB46*, were positively correlated with the neuroendocrine markers *SYP*, *CHGA* or *ENO2* in TCGA stomach adenocarcinoma (<http://www.cbioportal.org/>, Supplementary Table S4). A representative image of CNVs for 20q13.12-q13.2 is shown in Fig. 2B.

Using qPCR, we also demonstrated that the CN levels of *MYT1*, *NTSR1*, and *ZBTB46* in tumor tissue were higher than those in the matched control tissues from the 8 gastric amphicrine carcinomas ($P = 0.026$, 0.036 and 0.045 , respectively, Fig. 2C), consistent with their higher protein levels in tumor tissue (Fig. 2D).

Comparison of the copy number characteristics between gastric amphicrine carcinomas and MiNENs

To identify the similarities and differences in CNVs between amphicrine carcinoma and MiNEN, we collected both the CN variant genes in 8 amphicrine carcinomas and the CN variant genes in either the adenocarcinoma or the NEC component of 8 MiNENs that were previously investigated⁷. The average number of CN losses in amphicrine carcinomas was significantly less than that in the NEC component of MiNENs ($P = 0.007$), and CN gains in amphicrine carcinomas were slightly less than in the NEC component of MiNENs ($P = 0.060$). There was no statistically

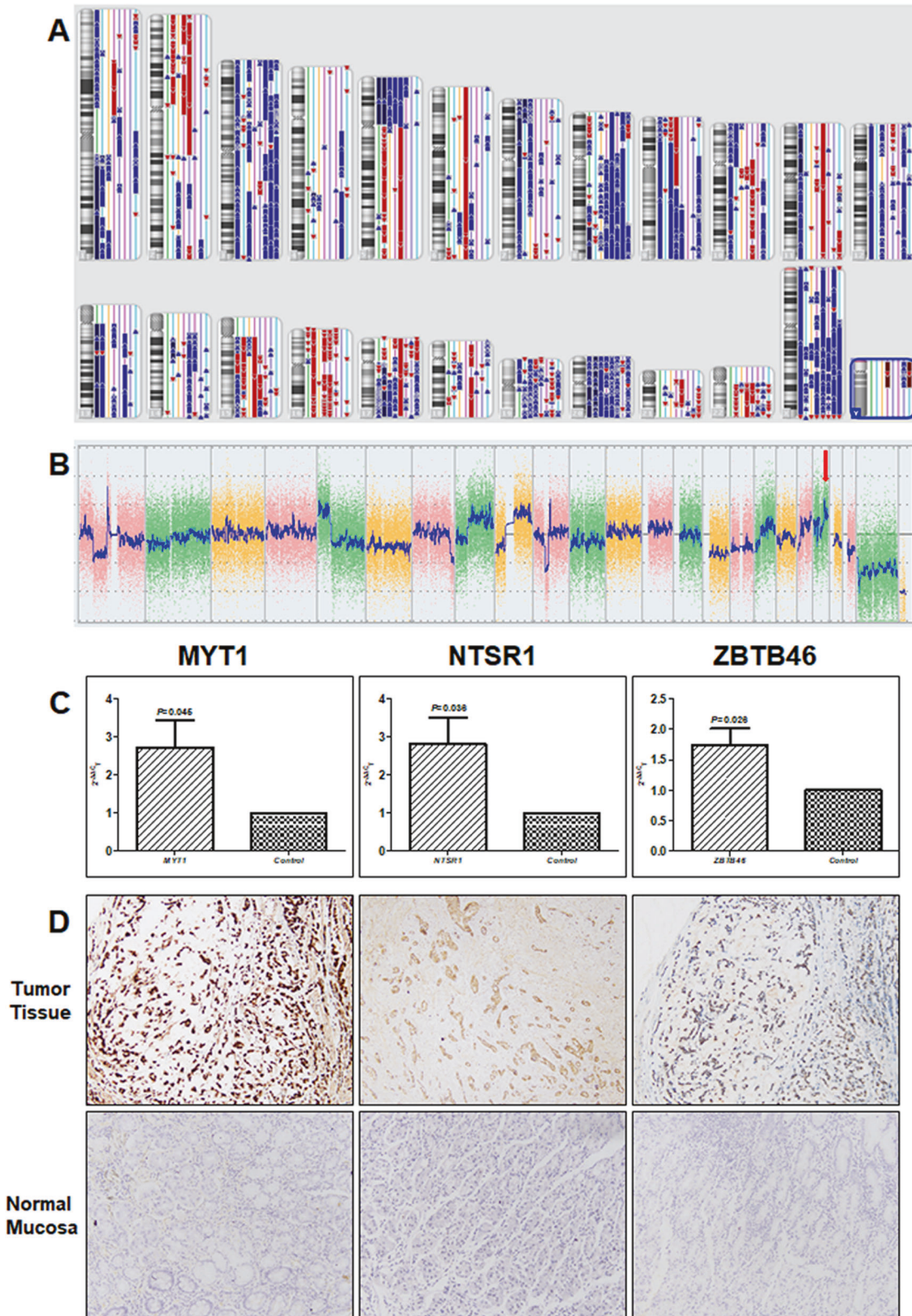


Fig. 2 Copy number variants (CNVs) in gastric amplicrine carcinomas. **a** An overview of CNVs in the eight gastric amplicrine carcinomas based on the results of an OncoScan CNV Assay. The chromosomes (1–22, X, and Y) are arranged in order. For each chromosome, the CNVs in eight cases are shown on the right (from left to right: case 1 to case 8). Blue bars indicate copy number gains, and red bars indicate copy number losses. **b** A typical case of gastric amplicrine carcinoma displaying gain of 20q13.12–q13.2 (red arrow, *MYT1*, *NTSR1*, and *ZBTB46* are localized in this region) discerned in the whole genome view. **c** qPCR validation of *MYT1*, *NTSR1*, and *ZBTB46* expression in eight gastric amplicrine carcinomas. The copy numbers of *MYT1*, *NTSR1*, and *ZBTB46* were significantly higher in carcinomas than in normal tissue. **d** Immunohistochemistry staining (200 \times) showed diffuse positive signals for *MYT1*, *NTSR1*, and *ZBTB46* in tumor cells, but no signal was observed in normal mucosa.

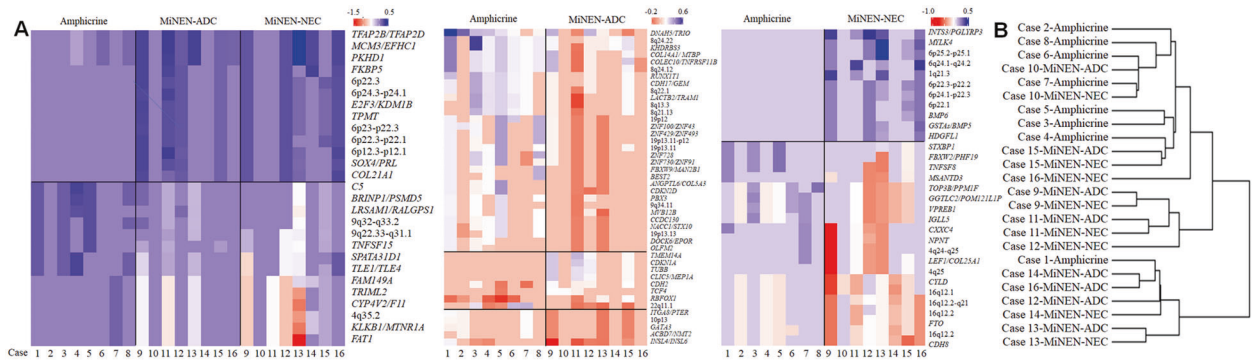


Fig. 3 CN level analysis of eight gastric amphicrine carcinomas as well as the adenocarcinoma and neuroendocrine components of eight gastric MiNENs. **a** Heatmap showing the different chromosomal regions and genes between amphicrine carcinomas and either component of MiNENs. The different chromosomal regions and genes between amphicrine carcinomas and both components of MiNENs (left panel); different chromosomal regions and genes between amphicrine carcinomas and the ADC component of MiNENs (middle panel); and different chromosomal regions and genes between amphicrine carcinomas and the NEC component of MiNENs (right panel). **b** Clustering analysis of all CNV genes in amphicrine carcinoma and MiNENs showed that amphicrine carcinoma tended to be clustered, except in case 1, while neither the adenocarcinoma nor the neuroendocrine component of MiNEN was clustered, except in case 10. Abbreviations: MiNEN, mixed neuroendocrine-non-neuroendocrine neoplasm; ADC, adenocarcinoma; NEC, neuroendocrine carcinoma.

significant difference in the average number of CN gains or losses between amphicrine carcinomas and the adenocarcinoma component of MiNENs.

There were no CN variant genes shared consistently among amphicrine carcinomas and both components of MiNENs. CN gain of *TSHZ2* (located at 20q13.2) was detected in 5 amphicrine carcinomas and the adenocarcinoma components of 4 MiNENs, followed by CN gains of 8q23.3 and 20p13-p11.21 identified in 4 amphicrine carcinomas and the adenocarcinoma components of 4 MiNENs. CN gain of 20q12-q13.2 was detected in 5 amphicrine carcinomas and the NEC component of 5 MiNENs, followed by 5p15.33-p14.3 in 5 amphicrine carcinomas and the NEC component of 4 MiNENs. No CN losses were shared among amphicrine carcinomas and either component of MiNENs.

We then compared the CN levels of all chromosomal regions and genes between amphicrine carcinomas and either component of MiNENs (Fig. 3A, $P < 0.05$). Among them, CN levels of genes located at 6p24.3-p12.1 [e.g., *MCM3* (6p12.2) and *E2F3* (6p22.3)] were lower in amphicrine carcinomas than in either component of MiNENs, and CN levels of genes located at 9q21.31-q34.11 and 4q35.1-q35.2 [e.g., *C5* (9q33.2) and *FAT1* (4q35.2)] were higher in amphicrine carcinomas than in either component of MiNENs (Fig. 3A left panel). CN levels of genes located at 6p22.1-p12.2, 16p13.3 and 18q12.1-q21.2 [e.g., *TUBB* (6p21.33), *CDKN1A* (6p21.2), *CDH2* (18q12.1) and *TCF4* (18q21.2)] were lower in amphicrine carcinomas than in adenocarcinoma components of MiNENs, and CN levels of genes located at 5p15.2, 8q13.3-8q24.23, 9p24.1, 9q33.3-q34.11, 10p14-p13, 19p13.2-p12, and 22q11.1 [e.g., *CDKN2D* (19p13.2) and *GATA3* (10p14)] were higher in amphicrine carcinomas than in adenocarcinoma components (Fig. 3A middle panel). CN levels of genes located at 1q21.3, 6p25.2-p12.1, and 6q24.1-q24.2 [e.g., *GSTAs*, *BMP5* (6p12.1) and *BMP6* (6p24.3)] were lower in amphicrine carcinomas than in NEC components, and CN levels of genes located at 4q24-q25, 9q31.1-q34.11, 16q12.1-q21, and 22q11.22 [e.g., *LEF1* (4q25) and *TOP3B* (22q11.22)] were higher in amphicrine carcinomas than in NEC components (Fig. 3A right panel).

Hierarchical clustering analysis showed that amphicrine carcinomas were clustered together except for case 1 (Fig. 3B). Except for one MiNEN (case 10), neither the adenocarcinoma nor the NEC component of MiNENs was clustered with amphicrine carcinoma (Fig. 3B).

The landscape of germline and somatic mutations in gastric amphicrine carcinoma

Both adjacent normal tissue and tumor tissue of the 8 gastric amphicrine carcinomas were analyzed to screen germline and somatically mutated genes. All cases presented a number of germline mutations, with an average number of 170 (range: 8–417). More germline mutations were detected in cases 1, 2, 3, 4, 5, and 6, while only a few germline mutations were detected in cases 7 and 8 (Fig. 4A). Among the germline mutations, *ZFXH3*, *MACF1*, and *PDE4DIP* (found in 6 cases) were the most frequently mutated genes, followed by *BRCA2*, *KMT2A*, *NCOA2*, *ARID1A*, *SEPT9*, and 8 other genes (found in 5 cases); *TSC2*, *LIFR*, and 34 other genes (found in 4 cases); and *TP53*, *MEN1*, *APC*, *CHD8* and 68 other genes (found in 3 cases).

One or more somatic mutations were detected in five cases (cases 1–4 and 8) (Fig. 4A). The average number of somatic mutations was 10 (range: 0–32). Among somatic mutations, *TP53* was the most frequently mutated, which was found in 3 cases (cases 1–3), followed by *APC*, *NEB*, and *EPPK1* ($n = 2$). Somatic mutations of *TP53* were validated by Sanger sequencing in the 3 cases (Fig. 4B). Immunohistochemical staining of p53 showed diffusely positive expression in cases 1 and 2, which was consistent with missense mutations of *TP53*, and negative expression in case 3, which was consistent with nonsense mutation of *TP53* (Fig. 4B).

Comparison of the mutation characteristics between gastric amphicrine carcinomas and MiNENs

We compared the mutation characteristics between the 8 amphicrine carcinomas and the two components of 7 MiNENs (WES results could not be obtained for case 15 due to an insufficient amount of DNA). All MiNENs presented a number of germline mutations (Fig. 4A), with an average number of 137 (range: 53–341). There was no significant difference in the number of germline mutations between amphicrine carcinomas and MiNENs ($P = 0.618$). Among the frequent germline mutations in amphicrine carcinomas, *PDE4DIP* and *ZFXH3* mutations were also frequent in MiNENs and were detected in 7 and 6 cases of MiNENs, respectively. *ARID1A* and *SEPT9* mutations were more frequent in amphicrine carcinomas than in MiNENs (for both genes, 5/8 vs. 0/7, $P = 0.026$), while *MUC20* and *DHX35* mutations were less frequent in amphicrine carcinomas than in MiNENs (2/8 vs. 6/7, $P = 0.041$ and 0/8 vs. 4/7, $P = 0.026$, respectively).

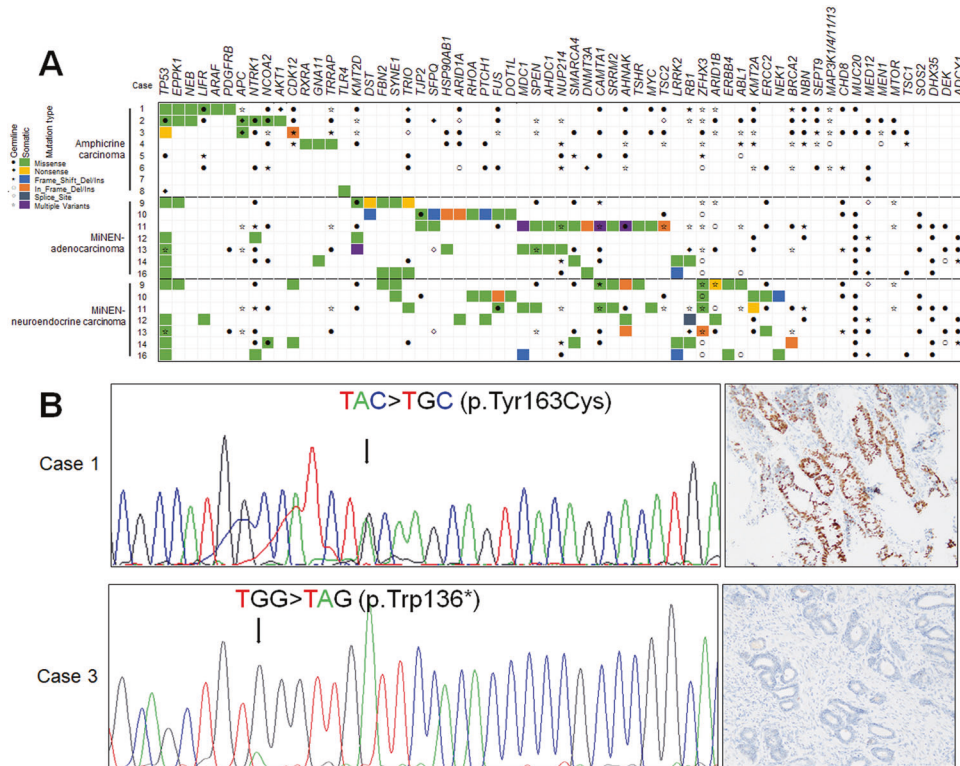


Fig. 4 Mutation landscapes of germline and somatic mutations in eight gastric amphicrine carcinomas and the adenocarcinoma and neuroendocrine components of seven gastric MiNENs. **a** Rows and columns represent cases and genes, respectively. Germline and somatic mutations are represented by different shapes or colors. For amphicrine carcinomas, rows represent case 1 to case 8 from top to bottom. For the adenocarcinoma and neuroendocrine components of MiNEN, rows represent case 9 to case 14 and case 16 from top to bottom. **b** Sanger sequencing analysis of *TP53* in case 1 and case 3. The arrows indicate the mutated nucleotides. Case 1 carries a heterozygous missense mutation (c.488 A > G, p. Tyr163Cys), and immunohistochemistry staining (200 \times) showed diffusely positive expression of p53; case 3 carries a heterozygous nonsense mutation (c.437 G > A, p. Trp136*), and immunohistochemistry staining (200 \times) was negative for p53. Abbreviation: MiNEN, mixed neuroendocrine-non-neuroendocrine neoplasm; #: Whole exome sequencing of MiNEN-case15 was not performed due to an insufficient amount of DNA.

The average number of somatic mutations was 19 (range: 6–33) and 23 (range: 9–52) in the adenocarcinoma and the NEC component of MiNENs, respectively (Fig. 4A). There was no significant difference in the number of somatic mutations among amphicrine carcinomas and the adenocarcinoma and NEC components of MiNENs ($P = 0.183$). Among the frequent somatic mutations in amphicrine carcinomas, *TP53* was also the most commonly mutated gene in MiNENs and was detected in both components of 5 MiNENs (Supplementary Table S5). *APC* and *NEB* mutations, the second most frequently mutated genes in amphicrine carcinomas, were not detected in either component of any MiNEN.

Integrated analysis of genetic characteristics in gastric amphicrine carcinomas and MiNENs

We collected all somatic mutated genes and highly frequent (at least in four cases) CN variant genes to perform an integrated KEGG pathway analysis. PI3K-Akt, MAPK, proteoglycans in cancer, oxytocin, Ras, focal adhesion, GnRH, regulating pluripotency of stem cells, estrogen, and transcriptional misregulation in cancer signaling pathways were the top 10 enriched signaling pathways ($P < 0.05$, Fig. 5). CN gains were predominantly observed in these enriched genes. *ADCY8*, *GNAS*, *NCOA3*, *NFATC2*, *PLCB1*, and *PLCB4*, which are involved in oxytocin and/or estrogen signaling pathways, and *ID1*, *MYC*, and *POU5F1B*, which are involved in signaling pathways regulating the pluripotency of stem cells, were the most frequent CN gains and were detected in seven cases at different levels. Loss of *AXIN1*, which is involved in signaling pathways regulating the pluripotency of stem cells, was the most frequent CN loss and was detected in five cases.

We also performed KEGG pathway analyses of the adenocarcinoma and NEC components of MiNENs using the same method. The estrogen signaling pathway was enriched in adenocarcinoma components, including gains of *ADCY8*, *GNAS*, *PLCB1*, and *PLCB4*, which were identified in both amphicrine carcinoma and adenocarcinoma components. Glutathione metabolism, TNF, and tight junction signaling pathways were enriched in adenocarcinoma components, including somatic mutation of *TJP2* and *RHOA*, gains of *TNFRSF1B*, and *TJAP1* and loss of *TRADD*, which were not detected in amphicrine carcinoma ($P < 0.05$, Supplementary Fig. 1A). The Ras, MAPK, oxytocin, and PI3K-Akt signaling pathways (including somatic mutation of *NTRK1*; gains of *RASAL2*, *NTRK1* and *EGFR*; and loss of *PLCB2* and *GNG13*) were enriched in NEC components, and these enrichments were also identified in amphicrine carcinoma. TGF-beta and TNF signaling pathways were enriched in NEC components but not enriched in amphicrine carcinomas, including somatic mutation of *ACVR2A* and *RHOA*, gains of *TRAF5*, and loss of *SMAD5*, *TRADD*, and *CASP3* ($P < 0.05$, Supplementary Fig. 1B).

DISCUSSION

For the first time, we report CNVs at 20q13.12-q13.2 and 15p13.33-q11.1 as the most common CN gains in amphicrine carcinoma. Among the genes located at 20q13.12-q13.2, *MYT1*, *NTSR1*, and *ZBTB46* might be associated with neuroendocrine differentiation. Myelin transcription factor 1 (*MYT1*) is an important islet cell transcription factor and forms a feed-forward expression loop with Ngn3 to promote endocrine islet cell differentiation⁸. Neurotensin

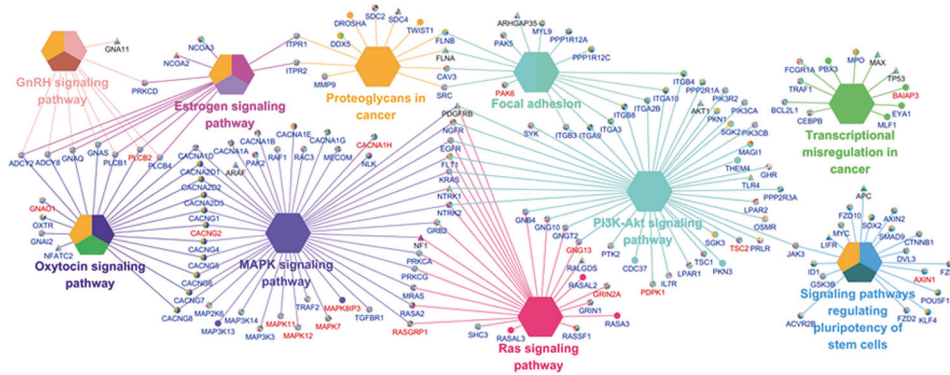


Fig. 5 Kyoto Encyclopedia of Genes and Genomes enrichment analysis of somatically mutated genes and frequent copy number variant genes in the eight gastric amphicrine carcinomas. The top 10 pathways (PI3K-Akt, MAPK, proteoglycans in cancer, oxytocin, Ras, focal adhesion, GnRH, regulating pluripotency of stem cells, estrogen, and transcriptional misregulation in cancer signaling pathways) are shown. Hexagon nodes represent the pathways; triangle nodes represent the mutated genes; nodes labeled in blue represent copy number gains, and nodes labeled in red represent copy number losses.

receptor 1 (*NTSR1*) belongs to the large superfamily of G-protein coupled receptors and mediates the multiple functions of neurotensin. High expression of *NTSR1* was found in gastrointestinal tract NET tissues, and knockdown of *NTSR1* in the human NET cell line BON suppressed its oncogenic functions, suggesting that *NTSR1* contributes to NET tumorigenesis⁹. In animal models of prostate cancer, *NTSR1* and *NTSR3* interact with their ligand *NTS* to activate downstream signaling and promote neuroendocrine differentiation¹⁰. Zinc finger and BTB domain containing 46 (*ZBTB46*) is a transcription factor. High expression of *ZBTB46* was responsible for the activation of LIF-STAT3 signaling and neuroendocrine-like features in prostate cancer cells¹¹. In this study, we validated the gain of *MYT1*, *NTSR1*, and *ZBTB46* using qPCR and demonstrated their high expression with immunohistochemical staining. The gain of 20q13.12-q13.2 and the relevant genes in this region deserve further study in gastric amphicrine carcinoma.

Furthermore, in the 8 gastric amphicrine carcinomas, we detected several frequent germline mutations, such as in *BRCA2*, *APC*, and *MEN1*, that are also frequent in other tumors. *MEN1* germline mutation has been reported in patients with hereditary and sporadic multiple endocrine neoplasia type 1 (*MEN1*) syndrome¹². However, in our study, the three patients with germline mutations of *MEN1* did not present with multiple endocrine neoplasms. We speculate that gastric amphicrine carcinoma might be the primary symptom of *MEN1* syndrome in the 3 patients, which should be investigated in the future. We did not find specific somatic mutations consistently shared across the 8 gastric amphicrine carcinomas. *TP53* somatic mutations were detected in three cases in which there were more somatic mutations than in the other five cases without *TP53* mutations, which is consistent with the function of *TP53* in DNA repair¹³.

Amphicrine carcinoma is characterized by typical ultrastructural exocrine (apical microvilli, tight junctions, and mucus granules) and endocrine features (dense core granules) present in the same tumor cells¹⁴. As a common amphicrine tumor, appendiceal goblet cell carcinoids share the same genetic alterations, such as *TP53* mutations, as appendiceal adenocarcinomas and appendiceal neuroendocrine tumors^{15, 16}. Meanwhile, some genes involved in chromatin remodeling (such as *ARID1A* and *KMT2D*) and signet-ring cell adenocarcinoma-related genes (such as *CDH1* and *RHOA*) were mutated in appendiceal goblet cell carcinoid tumors but not in appendiceal adenocarcinomas or appendiceal neuroendocrine neoplasms^{15, 17}. These data suggest that appendiceal goblet cell carcinoids show a distinctive mutational profile from appendiceal neuroendocrine tumors and conventional adenocarcinoma. Accordingly, appendiceal goblet cell carcinoid

was excluded from mixed adenoneuroendocrine carcinoma and renamed goblet cell adenocarcinoma in the 5th WHO classification of digestive system tumors because its behavior was more similar to that of appendiceal adenocarcinoma¹⁸. Similarly, gastric amphicrine carcinoma, which has been considered a subtype of mixed exocrine-neuroendocrine tumors^{3, 4} was also excluded from MiNENs in the 5th edition of the WHO classification of digestive system tumors⁵. Unfortunately, amphicrine carcinoma was not further classified or renamed. Although it was reported that gastric amphicrine carcinomas were clustered with conventional gastric adenocarcinomas but not neuroendocrine tumors (G1 and G2) based on pancancer transcriptome analysis in a limited series¹⁹, the genetic alterations and properties of gastric amphicrine carcinomas remain unclear.

In the present study, we compared the similarities and differences in genetic alterations between gastric amphicrine carcinomas and MiNENs. Although, in this study, *TP53* was the most common somatically mutated gene in both gastric amphicrine carcinomas and the two components of MiNENs, *TP53* mutation is also common in other types of tumors²⁰. The estrogen signaling pathway was shared by gastric amphicrine carcinomas and the adenocarcinoma component of MiNENs. The Ras, MAPK, oxytocin, and PI3K-Akt signaling pathways were shared by amphicrine carcinomas and the NEC component of MiNENs among their top 10 signaling pathways; however, these pathways are also frequently affected in other types of tumors. Except for a few CN gains detected in both amphicrine carcinomas and the adenocarcinoma or NEC component of MiNENs, there was an obvious difference in CNVs between amphicrine carcinomas and MiNENs. CN level analysis further demonstrated the differences between amphicrine carcinomas and either component of MiNENs. Interestingly, the CN level of C5 (complement C5) was higher in amphicrine carcinoma than in both the adenocarcinoma and NEC components of MiNENs, which suggests that amphicrine carcinomas might benefit more from C5 inhibitors than MiNENs.

Amphicrine carcinomas are considered clinicopathologically diverse. The 8 gastric amphicrine carcinomas examined in this study showed different degrees of differentiation, which is consistent with a previous report¹⁴. The overall survival time of gastric amphicrine carcinoma patients ranges from 11 months to 7 years and might be affected by histological grade, clinical stage, and treatment strategy^{19, 21}. Interestingly, in this study, all 8 patients with gastric amphicrine carcinoma were male, which was in line with the results reported by Huang¹⁹ et al. Our KEGG enrichment analysis of CNVs and mutated genes showed that oxytocin and estrogen signaling pathways were enriched in gastric amphicrine carcinomas, suggesting that sex hormones may

be involved in the development of this tumor. However, the gender distribution and related mechanisms need to be further investigated.

In summary, our study examined the clinicopathological features and revealed the CN and mutation characteristics of gastric amphicrine carcinoma and compared these characteristics with those of MiNENs. Due to its rarity, we only could analyze a small number of samples. We have yet to validate our hypotheses regarding amphicrine carcinoma on a mechanistic basis through in vitro and in vivo experiments. Nevertheless, our study, for the first time, outlined the genetic characteristics of gastric amphicrine carcinoma, identified candidate genes and signaling pathways that might be causally related to this tumor and provided new hints for further investigation.

DATA AVAILABILITY

The datasets used and/or analyzed during the current study are available from the corresponding author on reasonable request.

REFERENCES

- Ratzenhofer, M. Hyperplasias and tumors of the disseminated endocrine (paracrine) Helle Zellen Feyrter's of the gut with special regard of amphicrine cell proliferations (author's transl). *Verh. Dtsch. Ges. Pathol.* **61**, 7–24 (1977).
- Lewin, K. Carcinoid tumors and the mixed (composite) glandular-endocrine cell carcinomas. *Am. J. Surg. Pathol.* **11**(Suppl 1), 71–86 (1987).
- La Rosa, S., Marando, A., Sessa, F. & Capella, C. Mixed Adenoneuroendocrine Carcinomas (MANECs) of the gastrointestinal tract: an update. *Cancers* **4**, 11–30 (2012).
- de Mestier, L. et al. Digestive system mixed neuroendocrine-non-neuroendocrine neoplasms. *Neuroendocrinology* **105**, 412–425 (2017).
- Klimstra D. S., Klöppel G., La Rosa S., Rindi G. Classification of neuroendocrine neoplasms of the digestive system. In: WHO Classification of Tumors Editorial Board. Digestive System Tumors, WHO Classification of Tumors 5th Edition. 2019. p.16–19.
- Uccella, S. & La Rosa, S. Looking into digestive mixed neuroendocrine–non-neuroendocrine neoplasms: subtypes, prognosis, and predictive factors. *Histopathology* **77**, 700–717 (2020).
- Sun, L. et al. Chromosomal and molecular pathway alterations in the neuroendocrine carcinoma and adenocarcinoma components of gastric mixed neuroendocrine-non-neuroendocrine neoplasm. *Mod. Pathol.* **33**, 2602–2613 (2020).
- Wang, S. et al. Myt1 and Ngn3 form a feed-forward expression loop to promote endocrine islet cell differentiation. *Dev. Biol.* **317**, 531–540 (2008).
- Kim, J. T. et al. Differential expression and tumorigenic function of neurotensin receptor 1 in neuroendocrine tumor cells. *Oncotarget* **6**, 26960–26970 (2015).
- Zhu, S. et al. Neurotensin and its receptors mediate neuroendocrine transdifferentiation in prostate cancer. *Oncogene* **38**, 4875–4884 (2019).
- Liu, Y. N. et al. Leukemia inhibitory factor promotes castration-resistant prostate cancer and neuroendocrine differentiation by activated ZBTB46. *Clin. Cancer Res.* **25**, 4128–4140 (2019).
- Thakker, R. V. Multiple endocrine neoplasia type 1 (MEN1). *Best Pract. Res. Clin. Endocrinol. Metab.* **24**, 355–370 (2010).
- Zhou, J., Zhou, X. A., Zhang, N. & Wang, J. Evolving insights: how DNA repair pathways impact cancer evolution. *Cancer Biol. Med.* **17**, 805–827 (2020).
- Mandoky, L. Amphicrine tumor. *Pathol. Oncol. Res.* **5**, 239–244 (1999).
- Wen, K. W. et al. Genomic profile of appendiceal goblet cell carcinoid is distinct compared to appendiceal neuroendocrine tumor and conventional adenocarcinoma. *Hum. Pathol.* **77**, 166–174 (2018).
- Park, H. Y. et al. Targeted next-generation sequencing of well-differentiated rectal, gastric, and appendiceal neuroendocrine tumors to identify potential targets. *Hum. Pathol.* **87**, 83–94 (2019).
- Johncilla, M. et al. Mutational landscape of goblet cell carcinoids and adenocarcinoma ex goblet cell carcinoids of the appendix is distinct from typical carcinoids and colorectal adenocarcinomas. *Mod. Pathol.* **31**, 989–996 (2018).
- Misdraji J., Carr NJ, Pai R. K. Appendiceal goblet cell adenocarcinoma. In: WHO Classification of Tumors Editorial Board. Digestive System Tumors, WHO Classification of Tumors 5th Edition. 2019. p.149–151.
- Huang, D. et al. Amphicrine carcinoma of the stomach and intestine: a clinicopathologic and pan-cancer transcriptome analysis of a distinct entity. *Cancer Cell Int.* **19**, 310 (2019).
- Makuuchi, R. et al. Comprehensive analysis of gene mutation and expression profiles in neuroendocrine carcinomas of the stomach. *Biomed. Res.* **38**, 19–27 (2017).
- Fornelli, A. et al. Signet ring cell carcinoma of the ampulla of Vater with focal neuroendocrine differentiation of the amphicrine type: report of a case with long-term survival. *Int. J. Surg. Pathol.* **27**, 89–93 (2019).

FUNDING

This work was supported by grants from the National Natural Science Foundation of China (81871990 to Yan Sun).

AUTHOR CONTRIBUTIONS

Y.S. performed study concept and design; L.S., C.W., and Y.S. performed development of methodology and writing, review, and revision of the paper; L.S., C.W., J.Z., B.S., S.Z., Y.G., X.L. provided acquisition, analysis and interpretation of data, and statistical analysis. All authors read and approved the final paper.

ETHICS APPROVAL

This study was approved by the Institutional Review Board of Tianjin Medical University Cancer Institute and Hospital and is in compliance with the Helsinki Declaration.

CONFLICT OF INTEREST

The authors declare no competing interests.

ADDITIONAL INFORMATION

Supplementary information The online version contains supplementary material available at <https://doi.org/10.1038/s41379-021-00978-5>.

Correspondence and requests for materials should be addressed to Yan Sun.

Reprints and permission information is available at <http://www.nature.com/reprints>

Publisher's note Springer Nature remains neutral with regard to jurisdictional claims in published maps and institutional affiliations.